ELSEVIER

Journal of Organometallic Chemistry 549 (1997) 13–23

Journal of Organometallic Chemistry

A molecular structure of mixed valence biruthenocenium ($Ru^{II}Ru^{IV}$) salts $[Ru^{II}Cp(C_5H_4C_5H_4)CpRu^{IV}L]^{2+}(BF_4^-)_2$ ($L = NCCH_3$, $N(CH)_4N$)

Masanobu Watanabe [a,*], Izumi Motoyama [a], Toshio Takayama [a], Masaru Sato [b]

[a] *Department of Chemistry, Faculty of Engineering, Kanagawa University, Rokkakubashi, Yokohama 221, Japan*
[b] *Chemical Analysis Center, Saitama University, Urawa, Saitama 338, Japan*

Received 30 October 1996; received in revised form 26 March 1997

Abstract

The conformation of the oxidation product (**A**) of biruthenocene (RcRc) with *p*-benzoquinone containing boron trifluoride diethylether complex is $[RcRcC_6H_4O_2]^{2+}(BF_4^-)_2$ in which *p*-benzoquinoen is ligated to the Ru^{IV} center. The recrystallization of **A** from the mixture of nitromethane containing small amount of acetonitrile or pyrazine gives mixed-valence cations formulated as $[Ru^{II}Cp(C_5H_4C_5H_4)CpRu^{IV}L]^{2+}$ (L = acetonitrile **1** and pyrazine **2**), in which L is coordinated to the Ru^{IV} center. The crystal of **1** formulated as $[Ru^{II}Cp(C_5H_4C_5H_4)CpRu^{IV}NCCH_3]^{2+}(BF_4^-)_2 \cdot CH_3NO_2$ (**1**), is found to be orthorhombic, space group Pbca, a = 14.255(7), b = 37.105(10), c = 10.051(4) Å, V = 5316(4), Z = 8, and the final R = 0.054 and R_w = 0.059. The similar pyrazine salt **2** formulated as $[Ru^{II}Cp(C_5H_4C_5H_4)CpRu^{IV}N(CH)_4N]^{2+}(BF_4^-)_2(CH_3NO_2)_2$ is found to be triclinic, space group $P\bar{1}$, a = 9.006(2), b = 19.233(4), c = 28.907(10) Å, α = 89.45(1)°, β = 86.10(3)°, γ = 87.85(2)°, V = 4991(2), Z = 2, and the final R = 0.077 and R_w = 0.090. The unit cell has three independent molecules (**2A**, **2B**, **2C**). The Ru(IV)–N distances (2.15(1) Å for **2A**, 2.11(1) for **2B** and 2.15(1) for **2C**) are longer by ca. 0.1 Å than that of **1** because of bulky molecule of pyrazine. Both cations (**1**,**2**) have wedge-sharp structure due to the Ru–N bond, the dihedral angles between the Cp and C_5H_4 rings of the $[LRu^{IV}Cp(C_5H_4)]^{2+}$ moiety are 38.70° for **1**, 38.77° (**2A**), 40.84° (**2B**) and 41.67° (**2C**) for **2**. The nucleophilicity to the Ru^{IV} increases in the order Cl^- > pyrazine > acetonitrile > *p*-benzoquinone and unlike the case of mixed-valence halobiruthenocenium cations ($[RcRcX]^+$: X = Cl, Br, I), no temperature dependent ^1H – and ^{13}C-NMR spectra were observed for **1** and **2** in solution, implying the absence of two-electron exchange reaction between the Ru^{II} and Ru^{IV}. © 1997 Elsevier Science S.A.

Keywords: Metallocene; Ruthenocene; X-ray diffraction; Mixed-valence

1. Introduction

The chemistries of $[Ru(\eta^5\text{-}C_5H_5)(\eta^5\text{-}C_5H_4O)]^+$ and related compounds have been reported by Kirchner et al. [1]. Based on the results of the ^1H and ^{13}C-NMR studies, they concluded that there is strong interaction between the Ru and carbonyl group in the C_5H_4O ligand, resulting in higher oxidation state of Ru. Thus, the cation reacts with some nucleophiles (L) such as $AsMe_3$, $AsPh_3$, $P(OPh)_3$, CH_3CN giving pseudo-haloruthenocenium type cations $[RuCp(C_5H_4O)L]^+$ [1–3]. Recently, Ogino and co-workers reported the X-ray diffraction studies of interesting dicationic octamethyl [3]metallocenophanium salts prepared by the electrochemical oxidation in CH_3CN and formulated as $[C_5Me_4(CH_2)_3C_5Me_4M^{IV}NCCH_3]^{2+}$ in which the N atom of acetonitrile was coordinated to the M^{IV} (Ru, Fe) center in end-on form (the M^{IV}–N distance, 2.072 (6) for Ru; 1.916 (6) Å for Fe). Especially the latter Fe analogy is the first dicationic salt of ferrocene derivatives containing Fe^{IV} [4,5]. Although both groups' chemistries provide a great important information on the progress of the metallocene chemistry, their studies are within the range of mononuclear systems. Recently, binuclear metallocene chemistry plays an important role in the development of organometallic chemistry, because their chemical behaviors are differ significantly from those of analogous mononuclear complexes owing to a certain interaction between the central transition metals. The present authors have been reported the some mixed valence halobiruthenocenium cations ($RcRcX^+$) formulated as $[Ru^{II}Cp(C_5H_4C_5H_4)CpRu^{IV}X]^+$ with Ru^{IV}–X bond. On the results of tempera-

* Corresponding author.

PII S0022-328X(97)00230-1

ture dependent ^{1}H and ^{13}C-NMR spectroscopies [6–10], two-electron exchange reactions between the Ru^{II} and Ru^{IV} [$XRu^{IV}Ru^{II} \Leftrightarrow Ru^{II}Ru^{IV}X$] with X migration were observed and their activation energies are deeply concerned with the conformational change between the $Ru^{II}Cp(C_5H_4)$ and $[XRu^{IV}Cp(C_5H_4)]^+$ moieties based on the results of their X-ray diffraction studies (X = Cl, I) [6,7]. To extend our and above mentioned studies, two nonhalobiruthenocenium salts **1**, **2** formulated as $[Ru^{II}Cp(C_5H_4C_5H_4)CpRu^{IV}L]^{2+}(BF_4^-)_2$ with the Ru^{IV}–L bond have been prepared. Herein, these crystal structural and NMR studies are discussed as compared with those of reported $RcRcX^+$ and above two groups' salts.

2. Experimental

2.1. Syntheses

Salt **A** was prepared as follows; a solution of *p*-benzoquinone (30 mg) in hexane (100 ml) containing boron trifluoride diethyl ether complex (2 ml) was added to a solution of RcRc (50 mg, 0.11 mmol) in benzene (100 ml). Dark-brown precipitates were prepared (**A**) immediately in high yield (78 mg; 95%), see Scheme 1, which was filtered, washed with hexane and dried in vacuo. Anal. Found: C, 42.35; H, 2.84; $C_{26}H_{22}B_2F_8O_2Ru_2$. Calc.: C, 42.07; H, 2.99%. Infrared spectra (KBr): 3103, 1632, 1537, 1477, 1219, 1100–1000 (broad, BF_4^-), 875, 835, 762, 669, 530, 447 cm^{-1}. The precipitates **A** (78 mg) were well soluble in nitromethane (20 ml) containing small amount of acetonitrile (ca. 1 ml) giving a deep-red solution. Single crystals suitable for X-ray studies of **1** formulated as $[RcRcNCCH_3]^{2+}(BF_4^-)_2 \cdot CH_3NO_2$ were obtained by diffusion of diethyl ether into the solution at ca. 260 K for several days, the well-formed crystals (24 mg, 0.04 mmol; yield 36%) were obtained. Anal. Found: C, 37.49; H, 3.21; N, 3.58. $C_{23}H_{24}B_2F_8N_2O_2Ru_2$. Calc.: C, 37.52; H, 3.29; N, 3.81%. Infrared spectra (KBr): 3086, 1536, 1408, 1385, 1300, 1100–1000 (broad, BF_4^-), 843, 820, 667, 598, 434, 421 cm^{-1}. The salt **2** formulated as $[RcRcN(CH)_4N]^{2+}(BF_4^-)_2 \cdot (CH_3NO_2)_2$ was prepared by the same method for preparation of **1** by using pyrazine (ca. 50 mg) instead of acetonitrile. The well-formed red plane crystals were obtained (yield ca. 30%). Anal. Found: C, 37.42; H, 3.32.; N, 6.65. $C_{26}H_{28}B_2F_8N_4O_4Ru_2$. Calc.: C, 37.34; H, 3.37 N, 6.70%. Infrared spectra (KBr): 3095, 1636, 1485, 1410, 1300, 1100–1000 (broad, BF_4^-), 606, 534, 523, 469 cm^{-1}. The ^{1}H NMR and ^{13}C CP/MAS NMR measurements and dipolar dephasing experiments were carried out by the same method reported previously [11].

2.2. X-ray crystallography

Crystal ($0.2 \times 0.03 \times 0.5$ mm) of **1** was selected. X-ray intensities were recorded on a Rigaku AFC-6A automated four circle X-ray diffractometer with graphite mono-chromatized Mo-Kα radiation ($\gamma = 0.71073$ Å) at $25 \pm 1°$ using the $\omega - 2\theta$ scan mode with a scanning speed of 4° min. The lattice parameters were determined by a least-squares calculation with 25 reflections. Crystal stability was checked by recording three standard reflections every 150 reflection, and no significant vari-

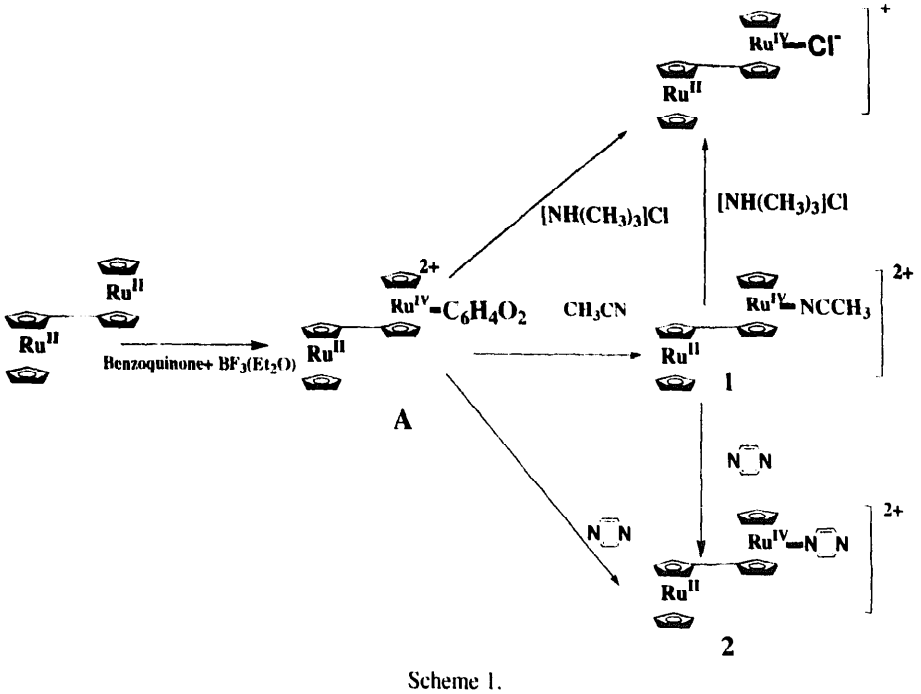

Scheme 1.

Table 1
Crystal and intensity collection data for **1** and **2**

	1	2
Formula	$C_{23}H_{24}Ru_2B_2F_8N_2O_4$	$C_{78}H_{84}Ru_6B_6F_{24}N_{12}O_{12}$
Formula weight	736.20	2508.54
Crystal dimensions (mm^3)	$0.2 \times 0.03 \times 0.5$	$0.1 \times 0.1 \times 0.2$
Space group	Pbca	$P\bar{1}$
a (Å)	14.255(7)	9.006 (2)
b (Å)	37.105(10)	19.233(4)
c (Å)	10.051(3)	28.907 (10)
α/°	-	89.45 (1)
β/°	-	86.10 (3)
γ/°	-	87.85 (3)
V (Å^3)	5316(4)	4991(2)
Z	8	2
T (K)	298	298
μ (cm^{-1})	12.18	9.90
D_x	1.840	1.669
No. of reflections measured	4089	22162
No. of observed reflections	1691($I > 1.5\ \sigma(I)$)	8992
2θ scan range (deg)	50.0	60
Scan width	$0.79 + 0.30 \tan\theta$	$1.15 + 0.30 \tan\theta$
p	0.033	0.04
R	0.054	0.077
R_w	0.059	0.090
(Δ/σ)max	0.01	0.00
$\Delta\rho$ min, $\Delta\rho$ max/eÅ^{-3}	−0.58,0.68	−0.97,1.88

ations were observed. For **1**, 4089 reflections were collected in the range $4° \leq 2\theta \leq 50°$ of which 1691 reflections with Iobsd > 1.5 σ(Iobsd) were used for the structure determination. The scan width was 0.79 + 0.3 tan θ. The refinement 352 variable parameters converged to $R = \Sigma||F_o| - |F_c||/\Sigma|F_o| = 0.054$, $R_w = [\Sigma w(|F_o| - F_c|)^2/\Sigma wF_o^2)]^{1/2} = 0.059$, and standard deviation of an observation of unit weight was 1.42.

For **2**, crystal ($0.1 \times 0.1 \times 0.2$) was selected. Due to the instability of **2**, the data were collected using a Mac Science MXC18K diffractometer with graphite monochromatized Mo-K α radiation ($\gamma = 0.71073$ Å) at 25 ± 1°, 22162 reflections were collected in the range $4° \leq 2\theta \leq 60°$ of which 8992 reflections with Iobsd > 2.5 σ (Iobsd) were used for the structure determination. The refinement 1380 variable parameters converged to $R = 0.077$, $R_w = 0.090$, and standard deviation of an observation of unit weight was 1.00.

Both structure (**1**, **2**) were solved by heavy-atom Patterson methods and expanded using Fourier techniques using the TEXSAN crystallographic software package [12]. The non-hydrogen atoms were refined anisotropically by full matrix least squares. All hydrogen atoms were located at the calculated positions, and were included isotropically in the refinement. Neutral atom scattering factors were taken from Cromer and Waber [13]; anomalous dispersion effects corrections were included in F_{cal} [14], the values for $\Delta f'$ and $\Delta f''$ were those of Creagh and McAuley [15]. Crystallographic data for **1** and **2** and some of the experimental conditions for the X-ray structure analysis are listed in Table 1.

3. Results and discussion

RcRc is oxidized by *p*-benzoquinone in benzene containing boron trifluoride diethyl ether complex giving intermediate salt **A**, this is well soluble in CH_3CN and other polar solvents giving deep-red solutions. From the ^{1}H-NMR spectrum in CD_3CN, the six-sharp signals (δ_H 6.24, 5.72, 5.71, 5.52, 5.32 and 4.90; ascribed to the $[Ru^{II}Cp(C_5H_4C_5H_4)CpRu^{IV}]^{2+}$ cation, the NMR discussion is described in latter) and one signal (δ_H 6.63) are observed. The latter δ_H is consistent with the value of free *p*-benzoquinone itself in the same conditions, thus **A** contains at least $RcRc^{2+}$ and *p*-benzoquinone. Fig. 1 shows ^{13}C CP/MAS NMR spectra of **A** (**a**), RcRc(**b**) and *p*-benzoquinone (**c**). Sharp three signals are observed for RcRc and the signal δ 87.5 is ascribed to the bridged C atom, δ 72.3 to Cp and $C_{2,5}$ and δ 69.1 to $C_{3,4}$ on the basis of our previous studies [8]. Two broad peaks (δ 187.1, 137.5) are observed for *p*-benzoquinone, the former is ascribed to the carbonyl and the latter is to olefine based on the result of ^{13}C NMR spectrum in solution (δ 187.3 and 136.6 in $CDCl_3$). Salt **A** gives five signals and the higher field two signals (δ 73.2, 76.5) are ascribed to the Cp and

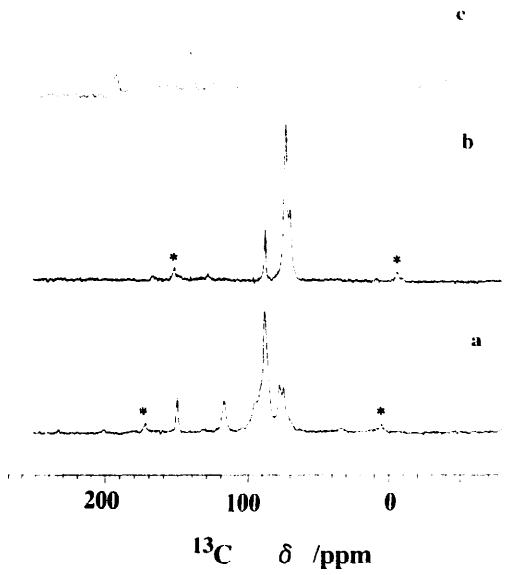

Fig. 1. ^{13}C cP/MAs NMR spectra of (a) **A**, (b) RcRc, and (c) *p*-benzoquinone. Spining side bands are marked with astetisks.

$C_{2,5}$ and $C_{3,4}$ of the $Ru^{II}Cp(C_5H_4)$ moiety and the signal (δ 89.0) and a shoulder (δ 93.1) are to those of the $[Ru^{IV}Cp(C_5H_4)]^{2+}$ moiety, respectively, on the results of our previous studies of $RcRcX^+$ [8]. The lower field two signals (δ 150.4, 117.8) are ascribed to the carbonyl and olefine C atoms of the *p*-benzoquinone, respectively, (the assignment of the signals is carried out by using the dipolar dephasing technique [11]). These large higher field shift (ca. 37, 20 ppm) compared with the values of the original *p*-benzoquinone suggests the reaction product **A** is a coordination complex of them, i.e., to fulfill the 18-electron rule of Ru^{IV}, *p*-benzoquinone is forced to ligate to the Ru^{IV} center of the $[Ru^{IV}Cp(C_5H_4)]^{2+}$ moiety, giving the $[Ru^{IV}Cp(C_5H_4)C_6H_4O_2]^{2+}$ fragment. From the infrared spectrum of **A**, the ν_{CO} signal is 1632 cm^{-1}, the signal shifts toward the lower frequency regions ca. 20 cm^{-1} compared with the value of free *p*-benzoquinone (ν_{CO} 1651 cm^{-1}). This red-shift is too small to consider the CO coordination to the Ru^{IV} center (Tuck et al. reported that the ν_{CO} band shifts to the ca. 1200–1400 cm^{-1} regions owing to the C–O–M character when the CO group of *o*-benzoquinone is ligated to the M atoms (M = In, Ga, Sn, Zn etc. [16]). A lack of success in preparing single crystals **A** of suitable size for the X-ray diffraction prevents the determination of the structure, however based on the results of the present studies (one kind of CO signal is found for the ^{13}C CP/MAS NMR spectrum and the elemental analysis data), the π-complex formulated as $[Ru^{II}Cp(C_5H_4C_5H_4)CpRu^{IV}C_6H_4O_2]^{2+}$ $(BF_4^-)_2$ in which π-electrons (2e) of the olefine in *p*-benzoquinone are ligated to the Ru^{IV} may be proposed for **A**. While in CH_3NO_2 solution of **A** containing small amount of CH_3CN, well-formed single crystals **1** suitable for X-ray diffraction were prepared and a detailed structural, NMR discussion of **1** will be presented in the latter section.

3.1. Structure of 1

The NMR and elemental analysis data of **1** suggest the conformation $[RcRcNCCH_3]^{2+}(BF_4^-)_2$. CH_3NO_2, the *p*-benzoquinone of **A** is easily substituted by CH_3CN in the solution, see Scheme 1. The crystal form of **1** is orthorhombic, space group Pbca and the final atomic coordinate and equivalent isotropic temperature factors of non-hydrogen atoms, select interatomic distance and angles for **1** are shown in Tables 2–4, respectively, and

Table 2
Atomic coordinates and isotropic temperature factors ($Å^2$) for **1**

Atom	*x*	*y*	*z*	B_{eq}^a($Å^2$)
Ru(1)	0.18439(9)	0.08710(3)	0.0996(1)	3.39
Ru(2)	−0.03364(9)	0.20561(3)	0.1299(1)	3.87
F(1)	0.291(1)	0.0781(5)	0.690(1)	15.9
F(2)	0.230(1)	0.0517(5)	0.518(2)	13.8
F(3)	0.3775(9)	0.0512(3)	0.539(2)	10.1
F(4)	0.303(1)	0.1009(4)	0.495(2)	13.5
F(5)	0.047(1)	0.1381(4)	0.699(1)	11.3
F(6)	−0.024(1)	0.1329(3)	0.504(1)	8.7
F(7)	0.0966(9)	0.1699(4)	0.525(1)	9.3
F(8)	−0.0357(10)	0.1831(3)	0.619(2)	11.0
O(1)	0.054(1)	0.0040(4)	0.802(2)	11.6
O(2)	−0.046(1)	0.0041(5)	0.655(2)	11.7
N(1)	0.2234(9)	0.1236(4)	−0.041(1)	4.3
N(2)	0.011(2)	0.0188(5)	0.718(2)	7.0
C(1)	0.330(1)	0.0697(6)	0.067(2)	6.0
C(2)	0.270(2)	0.0505(6)	−0.020(2)	5.7
C(3)	0.208(1)	0.0294(4)	0.057(3)	7.0
C(4)	0.232(2)	0.0373(6)	0.191(2)	5.9
C(5)	0.305(1)	0.0597(6)	0.192(2)	6.4
C(6)	0.083(1)	0. 1384(4)	0. 134(2)	3.2
C(7)	0.041(1)	0.1091(5)	0.064(2)	4.3
C(8)	0.039(1)	0.0799(4)	0.152(2)	5.2
C(9)	0.091(1)	0.0888(5)	0.268(2)	5.3
C(10)	0.121(1)	0.1246(4)	0.253(2)	4.4
C(11)	0.092(1)	0.1759(4)	0.090(2)	3.9
C(12)	0.055(1)	0. 1884(5)	−0.033(2)	5.0
C(13)	0.060(2)	0.2263(6)	−0.024(3)	7.1
C(14)	0.094(1)	0.2377(4)	0.099(3)	6.0
C(15)	0.115(1)	0.2057(5)	0.170(2)	5.0
C(16)	−0.145(1)	0. 1774(5)	0.237(3)	5.3
C(17)	−0.177(1)	0.1888(7)	0.112(2)	6.1
C(18)	−0.175(1)	0.2256(8)	0.114(3)	7.2
C(19)	−0.139(1)	0.2366(6)	0.238(3)	7.0
C(20)	−0.120(1)	0.2057(7)	0.312(2)	6.1
C(21)	0.241(1)	0.1421(4)	−0.127(2)	4.6
C(22)	0.267(1)	0.1652(5)	−0.238(2)	6.8
C(23)	0.032(1)	0.0560(6)	0.694(3)	9.2
B(1)	0.305(3)	0.0729(7)	0.571(3)	7.4
B(2)	0.020(2)	0.1545(7)	0.582(3)	5.8

[a] $Beq = 4/3(B_{11}a^2 + B_{22}b^2 + B_{11}c^2)$.
B_{ij} are defined by $\exp[-(h^2B_{11}k^2B_{22} + l^2B_{33} + 2klB_{23} + 2hlB_{13} + 2hkB_{12})]$.

Table 3
Select bond distances (Å) and bond angles (deg) for **1**

Bond distance			
Ru(1)–N(1)	2.04(2)	Ru(1)–C(1)	2.19(2)
Ru(1)–C(2)	2.19(2)	Ru(1)–C(3)	2.21(2)
Ru(1)–C(4)	2.17(2)	Ru(1)–C(5)	2.21(2)
Ru(1)–C(6)	2.41(1)	Ru(1)–C(7)	2.24(2)
Ru(1)–C(8)	2.15(2)	Ru(1)–C(9)	2.15(2)
Ru(1)–C(10)	2.27(2)	Ru(2)–C(11)	2.14(2)
Ru(2)–C(12)	2.16(2)	Ru(1)–C(13)	2.18(2)
Ru(2)–C(14)	2.20(2)	Ru(1)–C(15)	2.16(2)
Ru(2)–C(16)	2.18(2)	Ru(2)–C(17)	2.15(2)
Ru(2)–C(18)	2.15(2)	Ru(1)–C(19)	2.14(2)
Ru(2)–C(20)	2.20(2)	N(1)–C(21)	1.13(2)
C(21)–C(22)	1.45(2)	B(1)–F(1)	1.22(3)
B(1)–F(2)	1.44(2)	B(1)–F(3)	1.35(2)
B(1)–F(4)	1.29(2)	B(2)–F(5)	1.38(3)
B(2)–F(6)	1.28(3)	B(2)–F(7)	1.36(3)
B(2)–F(8)	1.37(3)		
Bond angles			
C(6)–Ru(1)–N(1)	74.7 (5)	C(1)–Ru(1)–N(1)	80.5(7)
C(2)–Ru(1)–N(1)	83.0(7)	C(21)–N(1)–Ru(1)	174(1)
C(22)–C(21)–N(2)	178 (2)	O(1)–N(2)–C(23)	117 (2)
O(1)–N(2)–O(2)	122 (2)	O(2)–N(2)–C(23)	120 (2)

ORTEP drawing of **1** is shown in Fig. 2 along with the atom numbering system. The cation of **1** is in trans conformation as with neutral RcRc and $RcRcX^+$ cations [6,7]. The Ru(1)···Ru(2) distance is found to be 5.393(2) Å, which is closer to the reported values of $Ru^{II}\cdots Ru^{IV}$ of $RcRcX^+$ (5.464(4) Å for X = I and 5.366(1) Å for Cl [6,7]) cations. The mean $Ru-C_{ring}$ (C_{ring}; C atoms of C_5H_4 and C_5H_5) and Ru–Cp (Ru–C_5H_5 and Ru–C_5H_4) distances are found to be 2.22(7), 1.87(1) Å for Ru(1) and 2.17(2), 1.82(1) Å for Ru(2), respectively, and the formal oxidation states of Ru(1) and Ru(2) must be assigned as Ru^{IV} and Ru^{II}, respectively, on the results of previous studies [6,7], i.e., the cation is formulated as $[Ru^{II}Cp(C_5H_4C_5H_4)Cp\text{-}Ru^{IV}NCCH_3]^{2+}$. The most interesting structural feature is found in the $[Ru^{IV}Cp(C_5H_4)NCCH_3]^{2+}$ moiety, i.e., the CH_3CN molecule (practically linear, the N–C(21)–C(22) angle; 178(2)°) is coordinated to the Ru^{IV} center in η^1-fashion (end-on form) as with Kirchener's and

Table 4
Selected Bond lengths (Å) of **1** and **2** and angles (deg)

	1	**2**		
		A	**B**	**C**
$Ru^{II}\cdots Ru^{IV}$	5.393 (2)	5.384 (4)	5.434 (3)	5.385 (3)
Ru^{II}–Cp	1.82(1)	1.81(1)	1.82(1)	1.82(1)
Ru^{IV}–Cp	1.87(1)	1.88(2)	1.87(1)	1.88(1)
$Ru^{II}-C_{ring}$	2.17(2)	2.17(3)	2.17(3)	2.17(3)
$Ru^{IV}-C_{ring}$	2.22 (7)	2.20 (9)	2.22 (8)	2.23 (9)
Ru–N	2.04(2)	2.15(1)	2.11(1)	2.15(1)
Dihedral angle of C_5H_4–$Ru^{IV}_5H_4$ C_5H_4–$Ru^{IV}C_5H_4$	38.70 2.20	38.77 3.13	40.84 3.10	41.67 3.03

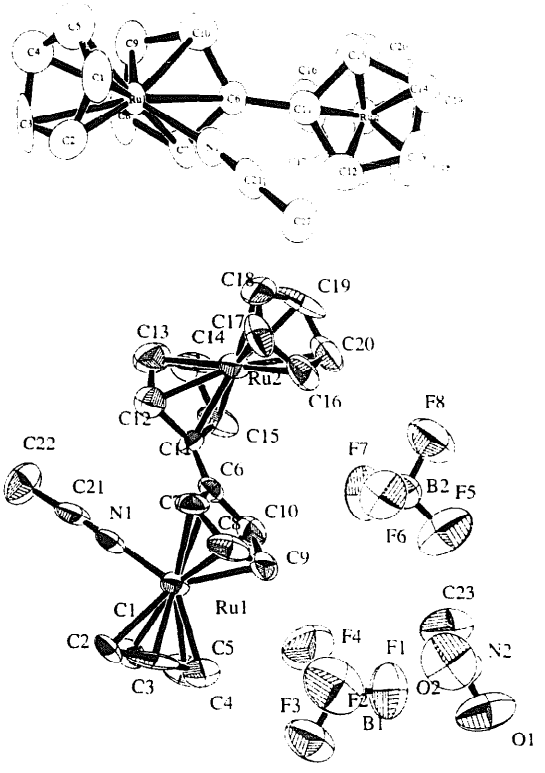

Fig. 2. ORTEP drawing of **1** with the thermal ellipsoids at the 40% probability level; perspective view with atomic numbering of the atoms (button), projection of a cation onto the Cp plane (top).

Ogino's and others $M-NCCH_3$ complexes [1–5,16–20]. The Ru^{IV}–N distance is 2.04(2) Å, which is the smallest one of all the values of the reported analogous ruthenocene–$NCCH_3$ complexes (e.g., 2.072(6) Å for $[C_5Me_4(CH_2)_3C_5Me_4Ru^{IV}NCCH_3]^{2+}$ [4], 2.064(7) Å for $[RuCp(C_5H_4OPPh_3)NCCH_3]^{2+}$ [3], 2.057(5) Å for $[RuCp(C_5H_4O)NCCH_3]^{2+}$ [2]). Although the M–N ≡ C angle is linear perfectly for $[C_5Me_4(CH_2)_3C_5Me_4M^{IV}NCCH_3]^{2+}$ (M = Ru, Fe) [4,5], the Ru(1)–N(1) ≡ C(21) angle is pseud-linear (the angle is 174(1)° which is closer to the value of $[RuCp(C_5H_4O)NCCH_3)]^{2+}$ (175.5(6)°) and other $M-NCCH_3$ complexes [17–20] probably because of steric hindrance between the CH_3CN and the $C_5H_4C_5H_4$ ligand.

The C ≡ N distance is 1.13(2) Å, which is significantly shorter than the value of free CH_3CN (1.1571 Å) [21]. It is well known that the C ≡ N distance is decreased when CH_3CN is coordinated to the metal atom in end-on form (e.g., 1.086(11) Å for $[C_5Me_4(CH_2)_3C_5Me_4Ru^{IV}NCCH_3]^{2+}$, 1.150(11) Å for $[C_5Me_4(CH_2)_3C_5Me_4Fe^{IV}NCCH_3]^{2+}$ and 1.133(7) Å for $[RuCp(C_5H_4O)NCCH_3)]^{2+}$), while the bond length is increased (1.200(10) and 1.211(10) Å for Cp_2MoCH_3CN [22]) when CH_3CN is coordinated to the metal atom in side-on form (η^2). Thus, the CN distance found in **1** is a reasonable one as an end form. In the infrared spectrum, the expected C ≡ N stretching

frequency is too weak to observe, as with Ogino's molecules $[C_5Me_4(CH_2)_3C_5Me_4M^{IV}NCCH_3]^{2+}$ [23]. The other interesting structural feature of the cation **1** compared with the reported $RcRcX^+$ is the direction of the Ru–$NCCH_3$ bond toward the $C_5H_4C_5H_4$ plane, as shown in Fig. 2; i.e., the CH_3CN molecule is coordinated to the Ru^{IV} from the oblique direction of the plane (the torsion angle N(1)–Ru(1)–C(6)–C(11); ca. 20°) owing to satisfy the closed packing described in detail later.

Because of the shorter Ru^{IV}–N distance of **1** compared with others M–$NCCH_3$ complexes, the Cp and C_5H_4 planes in Ru^{IV} side are slanted largely; the dihedral angle between the Cp and C_5H_4 planes is 38.7° (the Cp and C_5H_4 planes in Ru^{II} are almost parallel; the value is 2.20°), which is larger than the values of $[C_5Me_4(CH_2)_3C_5Me_4M^{IV}NCCH_3]^{2+}$ (34.5° for M–Fe and 34.83° for Ru) and $[RuCp(C_5H_3OPPh_3)NCCH_3]^+$ (35.5(7)° and closer to the value of mixed valence $[RcRcCl]^+$ (39.98°) [6].

Like the case of $RcRcX^+$, the much longer Ru(1)–C(6) distance (2.41(2) Å) compared with rest values of Ru–C (2.14–2.22 Å), nonplanarity of the C_5H_4 ligand of Ru^{IV} side (the dihedral angle between the C(6)–C(7)–C(10) and C(7)–C(8)–C(9)–C(10); 9.17°) and non-planarity of the $C_5H_4C_5H_4$ ligand (the dihedral angle between the C(6–10) and C(11–15); 17.04°) were observed. The phenomena were caused by the van der Waals repulsion between the N(1) and bridging carbon atoms (C(6), C(11)); i.e., the distance N(1)···C(6) (2.72(2) Å) and N(1)···C(11) (2.97(2) Å) are much smaller than the sum of the van der Waals radii (3.20 Å) of the N and C atom [24]), thus C(6) and C(11) atoms are located out of plane (C(6)–C(7)–C(10)–C(10)) largely, which gives above mentioned structural features.

A projection of the unit cell along the **c** axis of **1** is shown in Fig. 3. The cation is aligned along the **b** axis and piled along with **a** axis, these packing decides the direction of CH_3CN to the $Ru^{IV}CpC_5H_4$; i.e., the CH_3CN molecule is ligated to the Ru^{IV} from the oblique direction to reduce the intermolecular steric hindrance between the CH_3CN moiety and the BF_4^- when **1** is crystallized (although shortest intermolecular C(21)···–F and C(22)···F distances are 3.09(3) Å (F(1)) and 3.13(2) Å (F(8)), respectively, these values are closer to the sum (3.05 Å) of van der Waals radii of F and C, implying van der Waals contact between them. The CH_3NO_2 sits in a gap between the cations. The intramolecular distances of CH_3NO_2 are reasonable value; i.e., the C(23)–N(2), N(2)–O(1) and N(2)–O(2) distances are found to be 1.44(3), 1.19(2), 1.16(2) Å, respectively, and the C(23)–N(2)–O(1), C(23)–N(2)–O(2) and O(1)–N(2)–O(2) angles are 117(2), 120 (2) and 122 (2)°, respectively, and these values correspond well to those of free CH_3NO_2 (C–N (1.46 ± 0.02 Å), N–O (1.21 ± 0.02 Å) [25]. However, the two CH_3NO_2 molecules sit closer to each other (see in Fig. 3), the intermolecular shortest distance between them suggests no van der Waals contact, while the BF_4^- and CH_3NO_2 molecules are in van der Waals contact each other; i.e., the shortest F···C(23) distance is 3.05 Å (F(5)···C(23)) which corresponds to the sum of van der Waals radii of C and F. The average B–F distance is 1.34(7) Å, which is reasonable value as bonding distance.

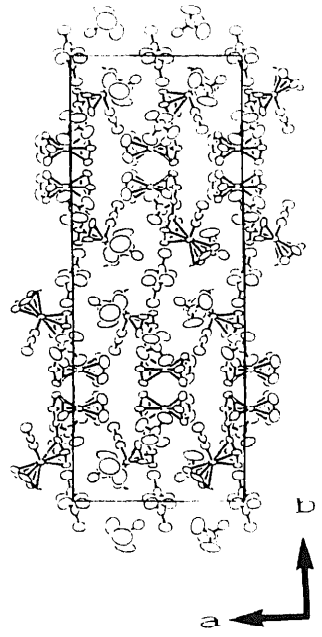

Fig. 3. Projection of the unit cell of **1** along with the *c* axis.

To investigate two-electron exchange reaction between the Ru^{II} and Ru^{IV} as with $RcRcX^+$, the NMR study was carried out for **1**. Salt **1** gives clear ^{1}H-NMR spectrum in CD_3COCD_3; i.e., six sharp ring proton signals are found; δ 6.64 (2H, t, α-position), 6.08 (5H, s, Cp), 6.02 (2H, t, β-position) for Ru^{IV} moiety and 5.81 (2H, t α-position), 5.67 (2H, t, β-position) and 5.00 (5H, s, Cp) for Ru^{II} moiety. The similar six lines (δ 6.24, 5.72, 5.71, 5.52, 5.32 and 4.90; they agreed with the values of **A** except for the free *p*-benzoquinone (δ 6.63); i.e., *p*-benzoquinone of **A** is easily substituted by CD_3CN giving **1**) were observed in CD_3CN although all signals shifted somewhat higher field owing to a higher dielectric constant of CD_3CN (ε; 37.5) compared with CD_3COCD_3(ε; 20.7)), and these δ values were summarized in Table 5. These δ values of ring-proton correspond well to the values of trapped-valence state of $RcRcX^+$ in the same solution (below ca. 200 K) reported by the present authors [8]; i.e., the formal oxidation states of two Ru are trapped-valence states ($Ru^{II}Ru^{IV}$) at 298 K. Upon heating of the samples (ca. 360 K), no significant broadening of the spectra were observed, which is in sharp contrast with the case of $RcRcX^+$, implying no electron exchange reaction between the Ru^{II} and Ru^{IV} for **1**.

Table 5
^{1}H NMR chemical shifts of **1** and **2**

	Chemical shift δ	Assignment
1a	6.24(t), 5.72(t)	$H_{2,5}$, $H_{3,4}$ position (Ru^{IV})
	5.71(s)	Cp-ring (Ru^{IV})
	5.52(t), 5.32(t)	$H_{2,5}$, $H_{3,4}$ position (Ru^{II})
	4.90 (s)	Cp-ring (Ru^{II})
	4.26(s)	CH_3NO_2
1b	6.64(t), 6.02(t)	$H_{2,5}$, $H_{3,4}$ position (Ru^{IV})
	6.08 (s)	Cp-ring (Ru^{II})
	5.81(t), 5.67(t)	$H_{2,5}$, $H_{3,4}$ position(Ru^{II})
	5.00 (s)	Cp-ring (Ru^{II})
	4.42 (s)	CH_3NO_2
	2.54(s)	CH_3CN
2b	9.18(d), 8.74(d)	pyrazine
	6.69(t), 6.09(t)	$H_{2,5}$, $H_{3,4}$ position (Ru^{IV})
	6.16 (s)	Cp-ring (Ru^{II})
	5.34(t), 5.24(t)	$H_{2,5}$, $H_{3,4}$ position (Ru^{II})
	4.88 (s)	Cp-ring (Ru^{II})
	4.42 (s)	CH_3NO_2

[a] In CD_3CN.
[b] In CD_3COCD_3.

The δ values of CH_3NO_2 and coordinated CH_3CN are found at δ 4.42 (3H, s) and 2.54 (3H, s) in CD_3COCD_3. The former is the reasonable value of free CH_3NO_2 in the some conditions, while the latter value is lowerfield ($\Delta\delta$) by ca. 0.6 ppm compared with the value of free CH_3CN. This $\Delta\delta$ is significantly smaller than the values of $[OsCp_2NCCH_3]^{2+}$ (ca. 0.9 ppm [26]), $[C_5Me_4(CH_2)_3C_5Me_4Ru^{IV}NCCH_3]^{2+}$ (ca. 0.9 ppm [4]) and $[CpC_5H_4ORu^{IV}NCCH_3]^{2+}$ (ca. 0.7 ppm [1]), implying somewhat weaker Ru^{IV}–$NCCH_3$ bond for **1** in solution compared with above three related complexes. Actually the CH_3-signal of the coordinated CH_3CN was not observed in CD_3CN solution because of fast exchange reaction between the coordinated CH_3CN and the solvent CD_3CN in solution, while the coordinated CH_3CN molecules does not exchange in CD_3CN for $[C_5Me_4(CH_2)_3C_5Me_4Ru^{IV}NCCH_3]^{2+}$ cation on the results of NMR studies of [4].

The coordinated *p*-benzoquinone of **A** and CH_3CN of **1** are easily substituted by Cl^- (using trimethylanrmonium chloride, see Scheme 1) and pyrazine giving mixed valence salts $[RcRcCl]^+BF_4^-$ and **2**, respectively, the former is determined by using elemental analysis, NMR and X-ray diffraction studies [6], and the detailed structural discussion of **2** is presented in the latter section.

3.2. Structure of 2

Pyrazine which contains two N atoms in *p*-position in the molecule, is a useful bridging ligand, which forms bi- or polynuclear complexes like Creutz–Taube mixed-valence ($Ru^{II}Ru^{III}$) complexes and many Cu-complexes [27–33]. The reason why pyrazine was selected as a ligand is to prepare related bridged complexes formulated such as $[Ru^{II}Cp(C_5H_4C_5H_4)CpRu^{IV}N(CH)_4NRu^{IV}Cp(C_5H_4C_5H_4)CpRu^{II}]^{4+}$. The salt **2** crystallized in the triclinic space group P1 and the final atomic coordinate and equivalent isotropic temperature factors of non-hydrogen atoms, select interatomic distance and angles for **2** are shown in Tables 4 and 6, and Table 7. The unit cell has three independent molecules (unit **2A**(Ru(1,2)), **2B**(Ru(3,4)) and **2C**(Ru(5,6), as shown in Fig. 4). Because of the three independent three cations and larger thermal motion of six BF_4^- anions and six CH_3NO_2 molecules (because of the thermal motion, the isotropic temperature factors of F in BF_4^- N and O atom in CH_3NO_2 are larger compared with the normal values, as shown in Table 6), the final *R* value is large, however the structural discussion of cation **2A** (the basic molecular structure of cation **2A** is quite similar to those of **2B** and **2C** (see Table 4)) is valuable in comparison with those of **1**.

The ORTEP drawings of the cations **2A** are shown in Fig. 5 along with the atom numbering system. The structure of **2A** is similar to that of **1**; i.e., pyrazine is ligated only to Ru(1) in the end-form and not bridged to two Ru atoms. This is the first pyrazine complex which structure determined by X-ray diffraction in ruthenocene analogies. Like the case of **1**, the cation takes trans conformation and the Ru(1)···Ru(2) distance is 5.384(4) Å. The mean $Ru–C_{ring}$ and Ru–Cp (C_5H_5, C_5H_4) distances are 2.20(9) and 1.88(2) Å for Ru(1) and 2.17(3) and 1.81(1) Å for Ru(2) see Table 4, respectively, which are closer to the corresponding values of **1**, and then the cation is formulated as $[Ru^{II}Cp(C_5H_4C_5H_4)CpRu^{IV}N(CH)_4N]^{2+}$ The N(1)–Ru(1) distance is 2.15(1) Å, which is longer by ca. 0.1 Å than the value of **1**.

Two structural features are found in **2** compared with that of **1**; one is larger tilting in the wedge-shape of the $[Ru^{IV}Cp(C_5H_4)]^+$ moiety in spite of much larger Ru^{IV}–N distance of **2**; the dihedralangles of Cp and C_5H_4 are 38.77° (40.84° for **2B** and 41.67° for **2C**, see Table 4). Nonplanality of the fulvalene ligand is also increased (the dihedral angle between the C_5H_4 planes is 18.33° (**2A**), which is larger by ca. 0.5° than the value of **1**). They may be caused by the balkiness of pyrazine than that of acetonitrile. The second is the coordinating direction of pyrazine molecule to the fulvalene ring; the pyrazine plane sits just above the C_5H_4 plane of the Ru^{II} side, as shown in Fig. 5, like the case of the reported $[RcRcX]^+BF_4^-$ salts [6,7]. This is probably because of absence of the intermolecular van der Waals contact between the coordinated pyrazine and BF_4^- CH_3NO_2. If this structure remains in solution, the ring current of coordinated pyrazine must influence to the δ of C_5H_4 in $Ru^{II}Cp(C_5H_4)$ moiety. Salt **2** gives the clear ^{1}H-NMR spectrum in acetone-d_6; i.e., six sharp ring protons are found at δ 6.69 (2H, t, α-position),

Table 6
Tables Atomic coordinates and isotropic temperature factors (Å^2) for **2**

Atom	x	y	z	B^a_{eq} (Å^2)
Ru(1)	0.0329(2)	0.25638(7)	0.30089(6)	4.96
Ru(2)	0.0925(2)	0.52442(7)	0.24994(5)	4.43
Ru(3)	0.2412(1)	0.07300(7)	0.60632(5)	4.17
Ru(4)	0.2962(2)	0.35314(7)	0.59472(5)	4.88
Ru(5)	0. 1356(1)	0.16423(7)	0.95559(5)	4.13
Ru(6)	0.1893(2)	0.43852(7)	0.92269(5)	4.12
F(1)	0.543(2)	0.062(2)	0.878(1)	19.9
F(2)	0.767(2)	0.033(1)	0.8873(8)	17.6
F(3)	0.599(5)	−0.015(1)	0.922(2)	40.0
F(4)	0.618(2)	0.083(1)	0.9427(7)	15.0
F(5)	0.386(2)	0.054(1)	0.4712(5)	12.3
F(6)	0.204(3)	0.002(1)	0.465(1)	24.8
F(7)	0.169(3)	0.097(2)	0.4599(8)	23.2
F(8)	0.280(2)	0.041(1)	0.4039(5)	16.9
F(9)	0.476(3)	0.075(2)	0.283(1)	24.1
F(10)	0.527(2)	0.179(1)	0.2920(7)	14.6
F(11)	0.422(2)	0. 135(2)	0.2316(7)	20.2
F(12)	0.658(2)	0.117(2)	0.2412(9)	22.2
F(13)	0.051(4)	0.167(2)	0.8055(8)	23.1
F(14)	0.049(3)	0.267(1)	0.7935(9)	21.3
F(15)	−0.077(4)	0.216(2)	0.754(1)	26.4
F(16)	0.122(4)	0.197(2)	0.7411(7)	25.2
F(17)	0.979(4)	0.316(2)	0.1442(6)	27.5
F(18)	0.817(3)	0.303(1)	0.108(2)	26.6
F(19)	0.982(4)	0.330(2)	0.0763(9)	22.2
F(20)	0.977(5)	0.242(2)	0.091(1)	27.4
F(21)	0.978(6)	0.331(2)	0.444(1)	35.4
F(22)	0.852(3)	0.389(2)	0.4835(7)	23.5
F(23)	0.773(5)	0.341(3)	0.426(1)	39.5
F(24)	0.893(3)	0.415(1)	0.4121(8)	19.5
O(1)	0.560(4)	0.172(1)	0.0627(9)	17.5
O(2)	0.746(3)	0.106(1)	0.059(1)	19.5
O(3)	0.643(3)	0.086(1)	0.7187(8)	15.6
O(4)	0.812(3)	0.023(1)	0.705(1)	18.5
O(5)	0.418(3)	0.324(2)	0.747(1)	22.6
O(6)	0.434(4)	0.009(2)	0.832(1)	28.6
O(8)	0. 111(4)	0.008(2)	0.762(1)	24.2
O(9)	0.347(4)	0.414(2)	0.410(2)	30.3
O(10)	0.204(5)	0.507(2)	0.390(1)	22.3
O(11)	0.298(3)	0.434(1)	0.092(2)	25.2
O(12)	0.379(4)	0.356(3)	0.129(2)	37.4
N(1)	−0.180(1)	0.301(1)	0.2853(5)	4.2
N(2)	−0.444(2)	0.362(1)	0.262(1)	11.0
N(3)	0.032(2)	0.1247(7)	0.6013(6)	5.1
N(4)	−0.242(2)	0.200(1)	0.594(1)	12.6
N(5)	−0.079(1)	0.2131(6)	0.9468(5)	3.8
N(6)	−0.343(2)	0.282(1)	0.936(1)	9.3
N(7)	0.641(3)	0.135(1)	0.080(1)	10.0
N(8)	0.710(4)	0.043(1)	0.7315(8)	12.2
N(9)	0.452(3)	0.297(2)	0.776(1)	12.2
N(10)	0.185(5)	0.024(2)	0.405(2)	16.1
N(11)	0.282(5)	0.459(2)	0.405(2)	16.0
N(12)	0.338(4)	0.392(1)	0.099(2)	21.2
C(1)	−0.051(3)	0.151(1)	0.291(1)	9.3
C(2)	−0.115(3)	0.177(1)	0.330(1)	11.2
C(3)	−0.006(4)	0.185(1)	0.360(1)	10.0
C(4)	0.130(3)	0.164(1)	0.335(1)	9.9
C(5)	0.099(3)	0. 144(1)	0.292(1)	8.9
C(6)	0.074(2)	0.3767(8)	0.2771(6)	4.6
C(7)	0.118(2)	0.358(1)	0.3226(7)	6.5
C(8)	0.237(2)	0.306(1)	0.313(1)	7.6

Table 6 (continued)

Atom	x	y	z	B^a_{eq} (Å^2)
C(9)	0.254(2)	0.287(1)	0.268(1)	7.6
C(10)	0.141(2)	0.325(1)	0.2461(8)	6.4
C(11)	−0.029(2)	0.4322(8)	0.2664(6)	4.3
C(12)	−0.082(2)	0.4873(8)	0.2983(6)	5.0
C(13)	−0.146(2)	0.5415(9)	0.2717(7)	5.6
C(14)	−0.135(2)	0.522(1)	0.2261(7)	5.6
C(15)	−0.059(2)	0.454(1)	0.2192(6)	5.2
C(16)	0.283(4)	0.564(3)	0.282(1)	18.2
C(17)	0.204(3)	0.620(1)	0.263(1)	10.4
C(18)	0.211(3)	0.610(1)	0.219(1)	7.4
C(19)	0.279(3)	0.554(2)	0.205(1)	10.2
C(20)	0.328(2)	0.516(1)	0.244(2)	12.2
C(21)	−0.267(2)	0.336(1)	0.3173(7)	5.5
C(22)	−0.400(2)	0.366(1)	0.306(1)	7.9
C(23)	−0.361(3)	0.330(1)	0.234(1)	8.8
C(24)	−0.226(2)	0.297(1)	0.2419(7)	6.7
C(25)	0.093(3)	−0.012(1)	0.626(1)	7.5
C(26)	0.149(3)	−9.022(1)	0.579(1)	7.5
C(27)	0.293(3)	−0.032(1)	0.577(1)	7.3
C(28)	0.335(3)	−0.030(1)	0.620(1)	8.4
C(29)	0.214(4)	−0.017(1)	0.6522(9)	9.9
C(30)	0.289(2)	0.1961(7)	0.6012(6)	4.1
C(31)	0.348(2)	0.1554(9)	0.5609(6)	5.1
C(32)	0.453(2)	0.107(1)	0.5758(9)	6.7
C(33)	0.453(2)	0.111(1)	0.624(1)	7.8
C(34)	0.338(2)	0.164(1)	0.6417(7)	6.1
C(35)	0.193(2)	0.2540(8)	0.5999(6)	4.7
C(36)	0.148(2)	0.290(1)	0.5574(7)	5.8
C(37)	0.064(2)	0.353(1)	0.5731(8)	6.2
C(38)	0.060(2)	0.359(1)	0.6210(9)	6.9
C(39)	0.139(2)	0.299(1)	0.6384(6)	6.2
C(40)	0.535(3)	0.352(2)	0.587(2)	13.4
C(41)	0.489(3)	0.391(2)	0.555(1)	10.5
C(42)	0.405(3)	0.448(1)	0.574(1)	8.7
C(43)	0.414(4)	0.438(2)	0.622(1)	10.6
C(44)	0.496(5)	0.379(2)	0.630(1)	17.4
C(45)	−0.024(2)	0.136(1)	0.5578(8)	7.2
C(46)	−0.164(3)	0.174(1)	0.557(1)	10.4
C(47)	−0.185(3)	0.185(1)	0.634(1)	11.2
C(48)	−0.046(2)	0.151(1)	0.6387(9)	7.2
C(49)	−0.009(3)	0.080(1)	0.978(1)	8.4
C(50)	0.091(4)	0.084(1)	1.009(1)	11.2
C(51)	0.233(3)	0.070(1)	0.987(1)	13.1
C(52)	0.210(3)	0.057(1)	0.941(1)	9.3
C(53)	0.055(3)	0.062(1)	0.935(1)	8.0
C(54)	0.176(2)	0.2889(8)	0.9399(6)	4.3
C(55)	0.224(2)	0.263(1)	0.9830(7)	6.2
C(56)	0.340(2)	0.210(1)	0.972(1)	7.3
C(57)	0.345(2)	0.200(1)	0.9238(9)	6.7
C(58)	0.239(2)	0.2414(9)	0.9052(6)	4.8
C(59)	0.072(2)	0.3442(8)	0.9337(6)	4.0
C(60)	0.020(2)	0.3926(9)	0.9678(6)	4.6
C(61)	−0.045(2)	0.450(1)	0.9455(7)	5.8
C(62)	−0.037(2)	0.438(1)	0.8982(7)	5.2
C(63)	0.038(2)	0.3726(8)	0.8883(6)	4.3
C(64)	0.429(2)	0.430(1)	0.921(1)	8.6
C(65)	0.389(3)	0.470(2)	0.955(1)	10.8
C(66)	0.306(2)	0.530(1)	0.936(1)	7.3
C(67)	0.313(2)	0.521(1)	0.8896(9)	6.9
C(68)	0.395(3)	0.461(2)	0.880(1)	8.8
C(69)	−0.156(2)	0.2416(9)	0.9817(7)	5.3
C(70)	−0.289(2)	0:276(1)	0.977(1)	7.5
C(71)	0.270(2)	0.254(1)	0.9005(9)	7.8

Table 6 (continued)

Atom	x	y	z	B_{eq}^{a} (Å^2)
C(72)	−0.133(2)	0.216(1)	0.9043(7)	6.1
C(73)	0.628(4)	0.130(1)	0.127(1)	11.1
C(74)	0.735(3)	0.040(2)	0.778(1)	11.2
C(75)	0.512(4)	0.235(2)	0.771(2)	19.2
C(76)	0.303(4)	0.070(2)	0.781(2)	25.4
C(77)	0.226(5)	0.472(4)	0.455(2)	24.5
C(78)	0.404(6)	0.357(3)	0.068(3)	22.2
B(1)	0.636(3)	0.049(3)	0.905(1)	16.5
B(2)	0.274(4)	0.060(2)	0.447(1)	9.5
B(3)	0.527(3)	0.143(3)	0.252(2)	17.5
B(4)	0.952(7)	0.312(6)	0.117(2)	29.4
B(5)	−0.010(9)	0.216(2)	0.781(2)	29.5
B(6)	0.801(9)	0.379(3)	0.451(2)	27.3

[a] Beq = $4/3(B_{11}a^2 + B_{22}b^2 + B_{11}c^2 + B_{13}ac\cos\beta + \beta_{12}a\,c\cos\gamma + B_{23}b\,c\cos\alpha)$.
$B_{ij}^{\wedge}$ are defined by exp $[-(h^2B_{11} + k^2B_{22} + l^2B_{33} + 2klB_{23} + 2hlB_{13} + 2hkB_{12})]$.

6.09 (2H, t, β-position), 6.16 (5H, s) for Ru^{IV} moiety and 4.88 (5H,s), 5.34 (2H, t, α-position) and 5.24 (2H,t, β-position) for Ru^{II} moiety. Although the former four δ values correspond well to the values of **1**, the latter two signals shift to the higher-field by 0.47 ppm for α-position and 0.43 ppm for β-position compared with the corresponding values of **1**. This suggests that the structure of the cation in solution keeps intact in the solid.

The δ difference (Δδ) of the Cp-ring of the Ru^{II} and Ru^{IV} moiety (Δδ; 1.08 ppm)is much larger than the value of **1** (Δδ; 0.81 ppm), implying that pyrazine is coordinated to the Ru^{IV} more stronger than CH_3CN. Actually, the treatment of **1** with pyrazine gave **2** immediately in acetone or nitromethane as demonstrated by the ^{1}H-NMR studies. Considering of the Δδ value of $RcRcCl^+$ cation (1.19 ppm [8]), the nucleophiiicity to the Ru^{IV} increases in the order Cl^- > pyrazine > acetonitrile > *p*-benzoquinone. The ring protons of coordinated pyrazine are found at δ 9.18 (2H, d), 8.74 (2H, d), they are shifted to lower field by 0.58 and 0.14 ppm compared with that of free pyrazine (δ 8.60), owing to the lowering of the electron density caused by the coordination of the N to the Ru^{IV} atom. The sharp signal at δ 4.42 is ascribed to the free CH_3NO_2. Like the case of **1**, no temperature dependency of the NMR spectra (no signal broading of Cp-ring protons and pyrazine's proton) was observed, implying no electron-exchange reaction between the Ru^{II} and Ru^{IV} in solution.

From the results in the present studies, it can be concluded that the formula of the oxidation product of RcRc with *p*-benzoquinone and boron trifluoride diethylether complex is $[Ru^{II}Cp(C_5H_4C_5H_4)CpRu^{IV}C_6H_4O_2]^{2+}(BF_4^-)_2$ in which *p*-benzoquinone is ligated to the Ru^{IV} center to fulfill the 18-electron rule of Ru^{IV}. The *p*-benzoquinone complex is easily substituted by acetonitrile or pyrazine giving the salts **1**, **2** formulated

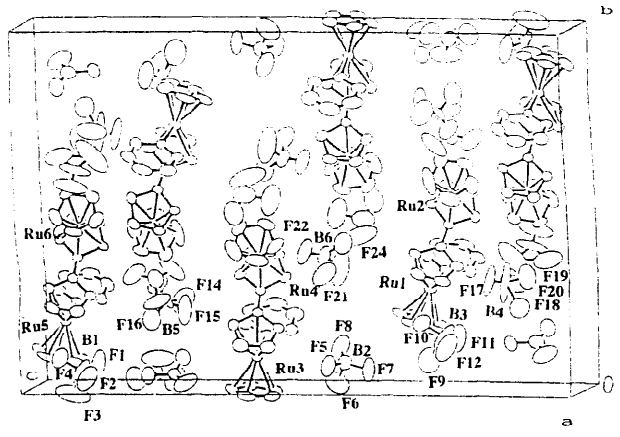

Fig. 4. Projection of the unit cell of **2**.

as $[Ru^{II}Cp(C_5H_4C_5H_4)CpRu^{IV}L]^{2+}$ with the Ru^{IV}–N bond. Both salts are soluble in polar organic solvents giving deep red solutions, the structure of the cations in solution remains intact in those of in solid. Unlike the case of $RcRcX^+$, no temperature dependency of the NMR spectra by the thermal process was found for **1**, **2**, suggesting absence of the electron-exchange reactions between the Ru^{II} and Ru^{IV}. The reason for the difference may be ascribed as follows; a higher positive Ru^{IV} charge may be delocalized easily through RuXRu (Ru^{II}

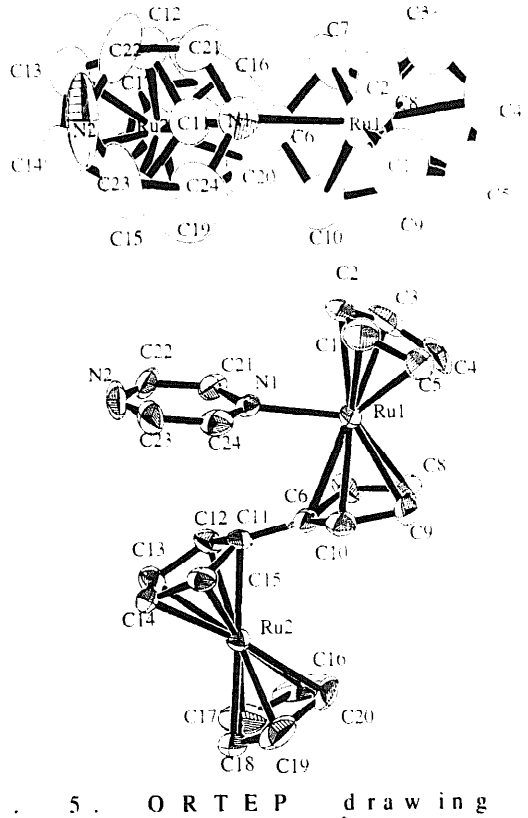

Fig. 5. ORTEP drawing of $[Ru^{II}Cp(C_5H_4C_5H_4)CpRu^{IV}N(C_2H_2)_2N]^{2+}$ cation at the 40% probability level; perspective view with the numbering of the atoms (button) and projection of a cation onto the Cp plane (top).

Table 7
Select bond distance (Å) for **2**

atom	atom	distance	atom	atom	distance
Ru(1)	N(1)	2.15(1)	Ru(2)	C(11)	2.15(2)
Ru(1)	C(1)	2.21(3)	Ru(2)	C(12)	2.17(2)
Ru(1)	C(2)	2.18(3)	Ru(2)	C(13)	2.21(2)
Ru(1)	C(3)	2.19(3)	Ru(2)	C(14)	2.21(2)
Ru(1)	C(4)	2.21(3)	Ru(2)	C(15)	2.19(2)
Ru(1)	C(5)	2.24(2)	Ru(2)	C(16)	2.17(4)
Ru(1)	C(6)	2.44(2)	Ru(2)	C(17)	2.17(3)
Ru(1)	C(7)	2.25(2)	Ru(2)	C(18)	2.15(2)
Ru(1)	C(8)	2.15(2)	Ru(2)	C(19)	2.14(3)
Ru(1)	C(9)	2.25(2)	Ru(2)	C(20)	2.11(2)
Ru(1)	C(10)	2.24(2)			
Ru(3)	N(3)	2.11(1)			
Ru(3)	C(25)	2.20(2)	Ru(4)	C(35)	2.15(2)
Ru(3)	C(26)	2.21(2)	Ru(4)	C(36)	2.18(2)
Ru(3)	C(27)	2.22(2)	Ru(4)	C(37)	2.1(2)
Ru(3)	C(28)	2.18(2)	Ru(4)	C(38)	2.1(2)
Ru(3)	C(29)	2.18(2)	Ru(4)	C(39)	2.13(2)
Ru(3)	C(30)	2.42(1)	Ru(4)	C(40)	2.15(3)
Ru(3)	C(31)	2.25(2)	Ru(4)	C(41)	2.16(3)
Ru(3)	C(32)	2.16(2)	Ru(4)	C(42)	2.17(2)
Ru(3)	C(33)	2.16(2)	Ru(4)	C(43)	2.17(3)
Ru(3)	C(34)	2.26(2)	Ru(4)	C(44)	2.20(4)
Ru(5)	N(5)	2.15(1)			
Ru(5)	C(49)	2.18(2)	Ru(6)	C(59)	2.14(2)
Ru(5)	C(50)	2.21(3)	Ru(6)	C(60)	2.15(2)
Ru(5)	C(51)	2.20(3)	Ru(6)	C(61)	2.17(2)
Ru(5)	C(52)	2.19(2)	Ru(6)	C(62)	2.20(2)
Ru(5)	C(53)	2.22(2)	Ru(6)	C(63)	2.19(2)
Ru(5)	C(54)	2.47(2)	Ru(6)	C(64)	2.15(2)
Ru(5)	C(55)	2.25(2)	Ru(6)	C(65)	2.19(3)
Ru(5)	C(56)	2.15(2)	Ru(6)	C(66)	2.14(2)
Ru(5)	C(57)	2.17(2)	Ru(6)	C(67)	2.15(2)
Ru(5)	C(58)	2.25(2)	Ru(6)	C(68)	2.21(2)
C(1)	C(2)	1.31(5)			
C(2)	C(3)	1.36(5)	C(1)	C(5)	1.36(4)
C(3)	C(4)	1.41(5)	C(4)	C(5)	1.38(5)
C(6)	C(7)	1.44(3)	C(6)	C(10)	1.44(3)
C(6)	C(11)	1.43(2)	C(7)	C(8)	1.45(3)
C(8)	C(9)	1.37(4)	C(9)	C(10)	1.41(3)
C(11)	C(12)	1.46(2)	C(11)	C(15)	1.46(2)
C(12)	C(13)	1.41(3)	C(13)	C(14)	1.37(3)
C(14)	C(15)	1.46(3)	C(16)	C(20)	1.46(5)
C(17)	C(18)	1.28(4)	C(18)	C(19)	1.29(4)
C(16)	C(17)	1.40(5)	C(19)	C(20)	1.42(5)
C(21)	C(22)	1.37(3)	C(25)	C(26)	1.43(4)
N(1)	C(21)	1.34(2)	N(1)	C(22)	1.35(3)
N(2)	C(22)	1.36(4)	N(1)	C(23)	1.22(4)
C(25)	C(29)	1.37(4)	C(25)	C(26)	1.43(4)
C(26)	C(27)	1.30(3)	C(27)	C(28)	1.34(5)
C(28)	C(29)	1.40(4)	C(30)	C(31)	1.47(2)
C(30)	C(34)	1.42(3)	C(30)	C(35)	1.39(2)
C(31)	C(32)	1.39(3)	C(33)	C(34)	1.49(3)
C(32)	C(33)	1.41(4)	C(35)	C(36)	1.48(3)
C(35)	C(39)	1.46(2)	C(36)	C(37)	1.46(3)
C(37)	C(38)	1.39(3)	C(38)	C(39)	1.43(3)
C(40)	C(41)	1.27(5)	C(40)	C(44)	1.36(6)
C(41)	C(42)	1.41(4)	C(42)	C(43)	1.41(4)
C(43)	C(44)	1.36(5)	C(45)	C(46)	1.44(3)
C(47)	C(48)	1.40(3)	N(3)	C(45)	1.40(3)
N(3)	C(48)	1.34(3)	N(4)	C(46)	1.38(4)
N(4)	C(47)	1.32(5)	C(49)	C(50)	1.32(5)
C(49)	C(53)	1.37(4)	C(50)	C(51)	1.40(5)
C(51)	C(52)	1.41(5)	C(52)	C(53)	1.41(4)

Table 7 (continued)

atom	atom	distance	atom	atom	distance
C(54)	C(55)	1.43(3)	C(54)	C(58)	1.44(2)
C(54)	C(59)	1.41(2)	C(55)	C(56)	1.44(3)
C(56)	C(57)	1.40(4)	C(57)	C(58)	1.35(3)
C(59)	C(60)	1.40(3)	C(59)	C(63)	1.47(2)
C(60)	C(61)	1.43(3)	C(61)	C(62)	1.39(3)
C(62)	C(63)	1.42(2)	C(64)	C(65)	1.27(4)
C(64)	C(68)	1.37(5)	C(65)	C(66)	1.47(4)
C(66)	C(67)	1.36(4)	C(67)	C(68)	1.37(4)
C(69)	C(70)	1.37(3)	C(71)	C(72)	1.41(3)
N(5)	C(69)	1.29(2)	N(5)	C(72)	1.35(2)
N(6)	C(70)	1.32(4)	N(6)	C(70)	1.32(4)

$\cdots X^{-} \text{———} Ru^{IV} \Leftrightarrow Ru^{IV} \text{———} X^{-} \cdots Ru^{II}$) for $RcRcX^{+}$, while the non-conjugated CH_3CN and the balkiness of pyrazine prevent the formation of conjugated $Ru^{II} \cdots L \text{---} Ru^{IV}$ species, and that gives the trapped valence ($Ru^{II}Ru^{IV}$) NMR spectra for **1** and **2**, however, further investigations are required in order to confirm this conclusions.

References

[1] K. Kirchner, K.S. Kwan, H. Taube, J. Chem. Soc. 113 (1991) 7039; K. Kirchner, K.S. Kwan, H. Taube, Inorg. Chem. 32 (1993) 4947; K. Kirchner, K. Mereiter, R. Schmid, J. Chem. Soc., Chem. Commun. (1994) 161; K. Kirchner, K. Merreiter, A. Umfahre, R. Schmid, Organometallics 13 (1994) 1886; K. Kirchner, K. Merreiter, K. Mauthner, R. Schmid, Organometallics 13 (1994) 3405; K. Mauthner, K. Merreiter, R. Schmid, K. Kirchner, Organometallics 13 (1994) 5054.

[2] K. Kirchner, K. Mereiter, R. Schmid, H. Taube, Inorg. Chem. 32 (1993) 1430.

[3] K. Kirchner, K. Mereiter, R. Schmid, H. Taube, Inorg. Chem. 32 (1993) 5553.

[4] K. Hashidzume, H. Tobita, H. Ogino, Organometallics 14 (1995) 1187.

[5] H. Ogino, H. Tobita, K. Hashidzume, M. Shimoi, J. Chem. Soc. Chem. Commun. (1989) 828.

[6] M. Watanabe, I. Motoyama, M. Shimoi, H. Sano, J. Organomet. Chem. 517 (1996) 115.

[7] M. Watanabe, I. Motoyama, M. Shimoi, T. Iwamoto, Inorg. Chem. 33 (1994) 2518.

[8] M. Watanabe, T. Iwamoto, A. Kubo, S. Kawata, H. Sano, I. Motoyama, Inorg. Chem. 31 (1992) 177.

[9] M. Watanabe, T. Iwamoto, H. Sano, I. Motoyama, J. Organomet. Chem. 442 (1992) 309.

[10] M. Watanabe, T. Iwamoto, H. Sano, I. Motoyama, J. Coord. Chem. 26 (1992) 223; M. Watanabe, T. Iwamoto, H. Sano, I. Motoyama, Inorg. Chem. 32 (1992) 5223.

[11] M. Watanabe, I. Motoyama, T. Takayama, M. Shimoi, H. Sano, J. Organomet. Chem. 496 (1995) 87.

[12] TEXSAN, Crystal Structure Analysis package, Molecular Structure Corporation, 1985.

[13] D.T. Cromer, J.T. Waber, International Table for X-ray Crystallography, Vol. IV, The Kynoch Press, Birmingham, UK, Table 2.2A (1974).

[14] J.A. Ibers, W.C. Hamilton, Acta Crystallogr. 17 (1964) 781.

[15] D.C. Creagh, W.J. McAuley, International Table for X-ray Crystallography, Vol. C, Kluwer Academic Publishers, Boston, Table 4.2.6.8, pp. 219-222, 1992.

[16] T.A. Annan, A. Ozarowski, Z. Tianand, D.G. Tuck, J. Chem. Soc. Dalton Trans. 2931 (1992); T.A. Annan, Z. Tian, D.G. Tuck, J. Chem. Soc. Dalton Trans. (1991) 19; M.K. Khan, R.C. Steevensz, D.G. Tuck, J.G. Noltes, P.W.R. Corfield, Inorg. Chem. 19 (1980) 3407.
[17] C. Landgrafe, W.S. Sheldrick, J. Chem. Soc., Dalton Trans. (1996) 989; W. Luginbuhl, P. Zbinden, P.A. Pittet, T. Armbruster, H.B. Btirgi, A.E. Merbach, A. Ludi, Inorg. Chem. 30 (1991) 2350.
[18] P.E. Riley, C.E. Capshew, R. Pettit, R.E. Davis, Inorg. Chem. 17 (1978) 408.
[19] M. Sato, K. Suzuki, H. Asano, M. Sekino, Y. Kawata, J. Organometal. Chem. 470 (1994) 263.
[20] S.A. Koch, M. Millar, J. Am. Chem. Soc. 105 (1983) 3362.
[21] C.C. Costain, J. Chem. Phys. 29 (1958) 864.
[22] T.C. Wright, G. Wilkinson, M. Motevalli, M.B. Hursthouse, J. Chem. Soc., Dalton Trans. (1986) 2017.
[23] Private Communication.
[24] L. Pauling, The Nature of the Chemical Bond, 3rd ed., Cornell University Press, 1960.
[25] E.H. Rodd, Chemistry of Carbon Compounds 1-A, Ch. 6, p. 357, 1951.
[26] M.W. Droege, W.D. Harman, H. Taube, Inorg. Chem. 26 (1987) 1309.
[27] P.A. Lay, H. Magnuson, H. Taube, Inorg. Chem. 27 (1988) 2364.
[28] C. Creutz, H. Taube, J. Am. Chem. Soc. 91 (1969) 3988.
[29] C. Creutz, H. Taube, J. Am. Chem. Soc. 95 (1973) 1086.
[30] M.J. Begley, P. Hubbeerstey, J. Stroud, J. Chem. Soc., Dalton, Trans. (1996) 2323.
[31] S. Kitagawa, M. Munakata, T. Tanimura, Inorg. Chem. 31 (1992) 1714.
[32] C.L. Klein, R.J. Majeste, L.W. Trefonas, C. O'Connor, Inorg. Chem. 21 (1982) 1891.
[33] S. Kitagawa, M. Munakata, T. Tanimura, Chem. Lett. (1991) 623.